Mathematical and Computational Applications, Vol. 15, No. 4, pp. 674-684, 2010.

TWO-DIMENSIONAL FLOW IN A DEFORMABLE CHANNEL WITH POROUS MEDIUM AND VARIABLE MAGNETIC FIELD

B. T. Matebese[1], A. R. Adem[1], C. M. Khalique[1] and T. Hayat[1,2]
[1]International Institute for Symmetry Analysis and Mathematical Modelling, Department of Mathematical Sciences, North-West University, Mafikeng Campus, Private Bag X2046, Mmabatho 2735, South Africa.
[2]Department of Mathematics, Quaid-i-Azam University, 45320 Islamabad, Pakistan.
katlinda@webmail.co.za, arademuv@gmail.com, Masood.Khalique@nwu.ac.za, pensy-t@yahoo.com

Abstract- This article is concerned with the analytic solution for a nonlinear flow problem of an incompressible viscous fluid. The fluid is taken in a channel having two weakly permeable moving porous walls. An incompressible fluid fills the porous space inside the channel. The fluid is magnetohydrodynamic in the presence of a time-dependent magnetic field. Lie group method is applied in the derivation of analytic solution. The effects of the magnetic field, porous medium, permeation Reynolds number and wall dilation rate on the axial velocity are shown and discussed.

Keywords- Porous medium, variable magnetic field, deformable channel.

1. INTRODUCTION

The two-dimensional flow of viscous fluid in a porous channel appears very useful in many applications. Hence many experimental and theoretical attempts have been made in the past. Such studies have been presented under the various assumptions like small Reynolds number R_e, intermediate R_e, large R_e and arbitrary R_e. The steady flow in a channel with stationary walls and small R_e has been studied by Berman [1]. Dauenhaver and Majdalani [2] numerically discussed the two-dimensional viscous flow in a deformable channel when $-50 < R_e < 200$ and $-100 < \alpha < 100$ (α denotes the wall expansion ratio). In another study, Majdalani *et al* [3] analyzed the channel flow of slowly expanding-contracting walls which leads to the transport of biological fluids. They first derived the analytic solution for small R_e and α and then compared it with the numerical solution.

The flow problem given in study [3] has been analytically solved by Boutros *et al* [4] when R_e and α vary in the ranges $-5 < R_e < 5$ and $-1 < \alpha < 1$. They used the Lie group method in this study. Mahmood *et al* [5] discussed the homotopy

perturbation and numerical solutions for viscous flow in a deformable channel with porous medium. Asghar *et al* [6] computed exact solution for the flow of viscous fluid through expanding-contracting channels. They used symmetry methods and conservation laws.

The purpose of this paper is to generalize the flow analysis of [4] into two directions. The first generalization is concerned with the influence of variable magnetic field while the second accounts for the features of porous medium. Like in [4], the analytic solution for the arising nonlinear flow problem is given by employing the Lie group method, with R_e and α as the perturbation quantities. Finally, the graphs for velocity and shear stress are plotted and discussed.

2. PROBLEM STATEMENT

We consider an incompressible and magnetohydrodynamic (MHD) viscous fluid in a rectangular channel with walls of equal permeability. An incompressible fluid saturates the porous space between the two permeable walls which expand or contract uniformly at the rate α (the wall expansion ratio). In view of such configuration, symmetric nature of flow is taken into account at $y = 0$. Moreover, the fluid is electrically conducting in the presence of a variable magnetic field $(0, \delta H(t), 0)$. Here δ is the magnetic permeability and H is a magnetic field strength. The induced magnetic field is neglected under the assumption of small magnetic Reynolds number. The physical model of the flow is shown in Figure 1.

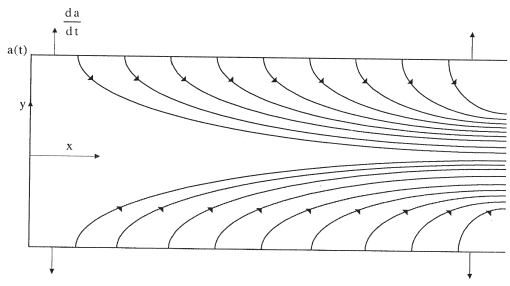

Figure 1: Coordinate system and bulk fluid motion

In view of the aforementioned assumptions, the governing equations can be written

as

$$\frac{\partial \bar{u}}{\partial \bar{x}} + \frac{\partial \bar{v}}{\partial \bar{y}} = 0, \tag{1}$$

$$\frac{\partial \bar{u}}{\partial t} + \bar{u}\frac{\partial \bar{u}}{\partial \bar{x}} + \bar{v}\frac{\partial \bar{u}}{\partial \bar{y}} = -\frac{1}{\rho}\frac{\partial \bar{P}}{\partial \bar{x}} + s\left[\frac{\partial^2 \bar{u}}{\partial \bar{x}^2} + \frac{\partial^2 \bar{u}}{\partial \bar{y}^2}\right]$$
$$-\frac{s\phi}{k}\bar{u} - \frac{r\delta^2 H^2(t)}{\rho}\bar{u}, \tag{2}$$

$$\frac{\partial \bar{v}}{\partial t} + \bar{u}\frac{\partial \bar{v}}{\partial \bar{x}} + \bar{v}\frac{\partial \bar{v}}{\partial \bar{y}} = -\frac{1}{\rho}\frac{\partial \bar{P}}{\partial \bar{y}} + s\left[\frac{\partial^2 \bar{v}}{\partial \bar{x}^2} + \frac{\partial^2 \bar{v}}{\partial \bar{y}^2}\right] - \frac{s\phi}{k}\bar{v}, \tag{3}$$

with the following conditions

$$\begin{aligned} &\text{(i)} && \bar{u} = 0, \quad \bar{v} = -V_w = -A\dot{a} \quad \text{at } \bar{y} = a(t), \\ &\text{(ii)} && \frac{\partial \bar{u}}{\partial \bar{y}} = 0, \quad \bar{v} = 0 \quad \text{at } \bar{y} = 0, \\ &\text{(iii)} && \bar{u} = 0 \quad \text{at } \bar{x} = 0. \end{aligned} \tag{4}$$

In above expressions $\bar{u}$ and $\bar{v}$ are the velocity components in $\bar{x}$ and $\bar{y}$-directions, respectively, ρ is the fluid density, $\bar{P}$ is the pressure, t is the time, s is the kinematic viscosity, ϕ and k are the porosity and permeability of porous medium, respectively, r is the electrical conductivity of fluid, V_w is the fluid inflow velocity, A is the injection coefficient corresponding to the porosity of wall and $\phi = V_f/V_c$ (where V_f and V_c, respectively, indicate the volume of the fluid and control volume).

The dimensional stream function $\overline{\Psi}(\bar{x}, \bar{y}, t)$ satisfies Eq.(1) according to the definitions of $\bar{u}$ and $\bar{v}$ given below

$$\bar{u} = \frac{\partial \overline{\Psi}}{\partial \bar{y}}, \qquad \bar{v} = -\frac{\partial \overline{\Psi}}{\partial \bar{x}},$$

which further takes the form

$$\bar{u} = \frac{1}{a}\frac{\partial \overline{\Psi}}{\partial y}, \qquad \bar{v} = -\frac{\partial \overline{\Psi}}{\partial \bar{x}}, \tag{5}$$

when $y = \bar{y}/a(t)$. Substituting Eq.(5) into Eqs.(2)-(4) and then relating the non-dimensional variables to the dimensional ones

$$u = \frac{\bar{u}}{V_w}, \quad v = \frac{\bar{v}}{V_w}, \quad x = \frac{\bar{x}}{a(t)}, \quad \Psi = \frac{\overline{\Psi}}{aV_w}, \quad P = \frac{\bar{P}}{\rho V_w^2},$$

$$\bar{t} = \frac{tV_w}{a}, \quad \alpha = \frac{a\dot{a}}{s}, \quad N = \frac{r\delta^2 a}{\rho V_w}, \quad \frac{1}{R} = \frac{s\phi a}{kV_w}, \tag{6}$$

we obtain

$$\Psi_{y\bar{t}} + \Psi_y\Psi_{xy} - \Psi_x\Psi_{yy} + P_x - \frac{1}{R_e}[\alpha\Psi_y + \alpha y\Psi_{yy} + \Psi_{xxy} + \Psi_{yyy}]$$

$$+\frac{1}{R}\Psi_y + NH^2(t)\Psi_y = 0, \tag{7}$$

$$\Psi_{x\bar{t}} + \Psi_y\Psi_{xx} - \Psi_x\Psi_{xy} - P_y - \frac{1}{R_e}[\alpha y\Psi_{xy} + \Psi_{xyy} + \Psi_{xxx}]$$

$$+\frac{1}{R}\Psi_x = 0 \tag{8}$$

and

$$\begin{aligned} &\text{(i)} \quad \Psi_y = 0, \quad \Psi_x = 1 \quad \text{at } y = 1, \\ &\text{(ii)} \quad \Psi_{yy} = 0, \Psi_x = 0 \quad \text{at } y = 0, \\ &\text{(iii)} \quad \Psi_y = 0 \quad \text{at } x = 0, \end{aligned} \tag{9}$$

where

$$u = \Psi_y, \qquad v = -\Psi_x \tag{10}$$

and subscripts denote the partial derivatives, N is the magnetic parameter, $R_e(= aV_w/s)$ is the permeation Reynolds number and R is porosity parameter. It should be pointed out that the present problem reduces to the problem studied in [4] when $N = 0$ and $R \to \infty$. Further $a\dot{a}$ = constant and $\alpha = a\dot{a}/s$, which implies that $a = (1 + 2.5\alpha t a_0^{-2})^{1/2}$. Here a_0 denotes the initial channel height.

3. SOLUTION

In this section we solve the present problem by following closely the Lie group method in [4] under which Eqs.(7) and (8) remain invariant. Following the methodology and notations in subsection (3.1) of [4] we note that the difference only occurs in the definitions of Δ_1 and Δ_2. In order to avoid repetition we only write the values of Δ_1 and Δ_2 here as

$$\begin{aligned} \Delta_1 &= \Psi_{y\bar{t}} + \Psi_y\Psi_{xy} - \Psi_x\Psi_{yy} + P_x - \frac{1}{R_e}[\alpha\Psi_y + \alpha y\Psi_{yy} + \Psi_{xxy} + \Psi_{yyy}] \\ &\quad +\frac{1}{R}\Psi_y + NH^2(t)\Psi_y, \\ \Delta_2 &= \Psi_{x\bar{t}} + \Psi_y\Psi_{xx} - \Psi_x\Psi_{xy} - P_y - \frac{1}{R_e}[\alpha y\Psi_{xy} + \Psi_{xyy} + \Psi_{xxx}] + \frac{1}{R}\Psi_x, \end{aligned} \tag{11}$$

where for other definitions and calculations, the readers may consult [4].

Now following the detailed procedure as given in [4] we finally obtain

$$
\begin{aligned}
&-K\frac{d^3h}{dy^3}+\Big[-\alpha Ky-hK_1-3KK_2\Big]\frac{d^2h}{dy^2}\\
&+\Big[-\alpha K-2\alpha KyK_2-hK_3+hK_4-KK_5-3KK_6+\frac{1}{R}+N\Big]\frac{dh}{dy}\\
&K_1\left(\frac{dh}{dy}\right)^2+\Big[-\alpha KK_2+\frac{1}{R}K_2+NK_2-\alpha KK_6y-KK_9-KK_{10}\Big]h\\
&+\Big[K_7-K_8\Big]h^2+\frac{1}{H}\frac{d\Gamma}{dx}=0,
\end{aligned}
\tag{12}
$$

where

$$
\begin{aligned}
&K_1=H_x,\quad K_2=\frac{H_y}{H},\quad K_3=\frac{H_xH_y}{H},\quad K_4=H_{xy},\\
&K_5=\frac{H_{xx}}{H},\quad K_6=\frac{H_{yy}}{H},\quad K_7=\frac{H_yH_{xy}}{H},\quad K_8=\frac{H_xH_{yy}}{H},\\
&K_9=\frac{H_{xxy}}{H},\quad K_{10}=\frac{H_{yyy}}{H},
\end{aligned}
\tag{13}
$$

with

$$
u=x\frac{dG}{dy},\quad v=-G \tag{14}
$$

and G satisfies

$$
\begin{aligned}
&\frac{d^4G}{dy^4}+\alpha\Big[y\frac{d^3G}{dy^3}+2\frac{d^2G}{dy^2}\Big]+R_eG\frac{d^3G}{dy^3}-R_e/R\ \frac{d^2G}{dy^2}-R_e\frac{d^2G}{dy^2}N\\
&-R_e\frac{dG}{dy}\frac{d^2G}{dy^2}=0
\end{aligned}
\tag{15}
$$

along with

$$
\text{(i)}\ \frac{dG(1)}{dy}=0,\quad \text{(ii)}\ G(1)=1,\quad \text{(iii)}\ \frac{d^2G(0)}{dy^2}=0,\quad \text{(iv)}\ G(0)=0 \tag{16}
$$

and $K=R_e$. Writing

$$
\begin{aligned}
G &= G_1+R_eG_2+R_e^2G_3+0(R_e^3),\\
G_1 &= G_{10}+\alpha G_{11}+\alpha^2G_{12}+0(\alpha^3),\\
G_2 &= G_{20}+\alpha G_{21}+\alpha^2G_{22}+0(\alpha^3),\\
G_3 &= G_{30}+\alpha G_{31}+\alpha^2G_{32}+0(\alpha^3),
\end{aligned}
$$

we solve the problem consisting of equation (15) and conditions given in (16) using second-order double perturbation and finally arrive at

$$\begin{aligned}
G_1(y) &= \frac{1}{2800}\Big[y(-(25y^2-13)(y^2-1)^2\alpha^2+210(y^2-1)^2\alpha \\
&\quad -1400(y^2-3))\Big], \\
G_2(y) &= \frac{1}{232848000R}\Big[y(y^2-1)^2(831600(R(-7\mathrm{N}+y^2+2)-7) \\
&\quad -2310\alpha(-2y^2((240\mathrm{N}-227)R+240)+(552\mathrm{N}+681)R+65Ry^4 \\
&\quad +552)+\alpha^2(-35y^4((3905\mathrm{N}-6561)R+3905)+2y^2((133595\mathrm{N} \\
&\quad +50481)R+133595)-3((29953\mathrm{N}+114111)R+29953) \\
&\quad +12600Ry^6))\Big], \qquad (17)
\end{aligned}$$

$$\begin{aligned}
G_3(y) &= \frac{y(y^2-1)^2}{1271350080000R^2}\Big[1260\alpha(R^2(1001\mathrm{N}^2(5y^2-9)(25y^2-37) \\
&\quad -26\mathrm{N}(875y^6+18305y^4+293y^2-51137) \\
&\quad -4060y^8+63133y^6+357696y^4+427177y^2+394166) \\
&\quad +26R(77\mathrm{N}(5y^2-9)(25y^2-37)-875y^6-18305y^4-293y^2 \\
&\quad +51137)+1001(5y^2-9)(25y^2-37))+\alpha^2(105Ry^8((6510\mathrm{N} \\
&\quad -46873)R+6510)-42y^6(R(350\mathrm{N}((1339\mathrm{N}-7698)R+2678) \\
&\quad +3099111R-2694300)+468650)+14y^4(R(900\mathrm{N}((6552\mathrm{N} \\
&\quad -10585)R+13104)-2957491R-9526500)+5896800) \\
&\quad -y^2(R(84\mathrm{N}((1262105\mathrm{N}+3260532)R+2524210) \\
&\quad -95806709R+273884688)+106016820)R+3R(42\mathrm{N}((245908\mathrm{N} \\
&\quad +2413431)+491816)+100425529R+101364102)+783825R^2y^{10} \\
&\quad +30984408)+491400(R(7y^4((55\mathrm{N}-102)R+55)-2y^2(77\mathrm{N}(\\
&\quad (10\mathrm{N}-23)R+20)+530R)+77\mathrm{N}((44\mathrm{N}+69)R+88) \\
&\quad +28Ry^6-1406R+1771(2y^2+3))+308(11-5y^2))\Big]. \qquad (18)
\end{aligned}$$

It can be easily noted that for $N = 0$ and $R \to \infty$, $G(y)$ reduces to the result presented in [4], provided we use a first-order double perturbation. This shows confidence in the present calculations. The shear stress at the wall with $y = 1$ is [4]

$$\tau_w = Kx\frac{d^2G(1)}{dy^2}. \qquad (19)$$

The velocity components through Eqs.(14) and (18) are given by

$$u = x\frac{dG}{dy}, \tag{20}$$

$$v = -G. \tag{21}$$

4. RESULTS AND DISCUSSION

4.1. Self-axial velocity

Figures 2 and 3 demonstrates the behaviour of the self axial velocity u/x for magnetic parameter $N = 0.5$, porosity parameter $R = 0.5$, permeation Reynolds number $R_e = -1$ and 1, at $-1 \leq \alpha \leq 1$. Figure 2 shows the case of $R_e = -1$. When $\alpha > 0$, the flow towards the centre becomes greater, this leads to the axial-velocity to be greater near the centre. We noticed that this behaviour changes when $\alpha < 0$, that is, the flow towards the centre results in lower axial velocity near the centre and higher near the wall. Similarly conclusions can be made for figure 3, when $R_e = 1$, we have the same pattern as in figure 2.

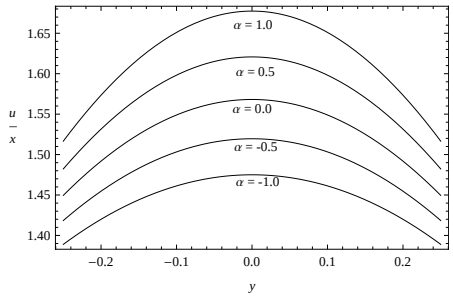

Figure 2: Self-axial velocity profiles over a range of α at $N = 0.5$, $R_e = -1$ and $R = 0.5$

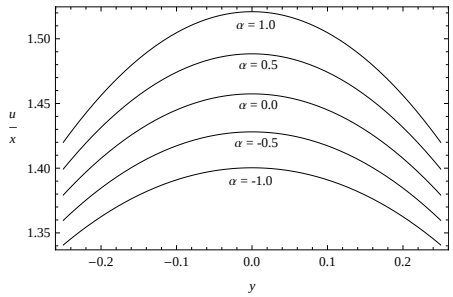

Figure 3: Self-axial velocity profiles over a range of α at $N = 0.5$, $R_e = 1$ and $R = 0.5$

From the figures above, we can see that the behaviour of the graphs is a cosine profile. Comparing analytical and numerical solutions, the percentage error increases as N increases for all $|\alpha|$, see Tables 1, 2 and 3.

Table 1: Comparison between analytical and numerical solutions for self-axial velocity u/x at $y = 0.3$ for $R = 0.5, R_e = -1, \alpha = -0.5$.

	Analytical Method	Numerical Method	Percentage Error (%)
N= 0.5	1.374237	1.375731	0.108609
$N = 1.0$	1.381895	1.384237	0.169198
$N = 1.5$	1.389799	1.393274	0.249420

Table 2: Comparison between analytical and numerical solutions for self-axial velocity u/x at $y = 0.3$ for $R = 0.5, R_e = -1$ and $\alpha = 0.0$.

	Analytical Method	Numerical Method	Percentage Error (%)
$N = 0.5$	1.398273	1.400185	0.136611
$N = 1.0$	1.406663	1.409625	0.210186
$N = 1.5$	1.415323	1.419678	0.306770

Table 3: Comparison between analytical and numerical solutions for self-axial velocity u/x at $y = 0.3$ for $R = 0.5, R_e = -1$ and $\alpha = 0.5$.

	Analytical Method	Numerical Method	Percentage Error (%)
$N = 0.5$	1.423053	1.425483	0.170456
$N = 1.0$	1.432188	1.435905	0.258803
$N = 1.5$	1.441616	1.447026	0.373840

For porosity parameter R, the axial velocity and the percentage error between analytical and numerical solutions decreases as R increases, for the same $|\alpha|$, see Tables 4, 5 and 6.

Table 4: Comparison between analytical and numerical solutions for self-axial velocity u/x at $y = 0.3$ for $N = 0.5, R_e = -1$ and $\alpha = -0.5$.

	Analytical Method	Numerical Method	Percentage Error (%)
$R = 0.5$	1.374237	1.375731	0.108609
$R = 1.0$	1.359664	1.360126	0.033979
$R = 1.5$	1.355025	1.355296	0.019936

Table 5: Comparison between analytical and numerical solutions for self-axial velocity u/x at $y = 0.3$ for $N = 0.5, R_e = -1$ and $\alpha = 0.0$.

	Analytical Method	Numerical Method	Percentage Error (%)
$R = 0.5$	1.398273	1.400185	0.136611
$R = 1.0$	1.382302	1.382914	0.044241
$R = 1.5$	1.377219	1.377581	0.026294

Table 6: Comparison between analytical and numerical solutions for self-axial velocity u/x at $y = 0.3$ for $N = 0.5, R_e = -1$ and $\alpha = 0.5$.

	Analytical Method	Numerical Method	Percentage Error (%)
$R = 0.5$	1.423053	1.425483	0.170456
$R = 1.0$	1.405658	1.406468	0.057581
$R = 1.5$	1.400120	1.400610	0.035000

4.2. Shear stress

Figures 12, 13 and 14 illustrate the effects of varying governing parameters on the character of the shear stress at the wall. For a suction-contracting process ($Re = -1$ and $\alpha < 0$), the shear stress is positive until expansion is sufficiently large, while for a suction-expansion process ($Re = 1$ and $\alpha > 0$) the shear stress turns negative.

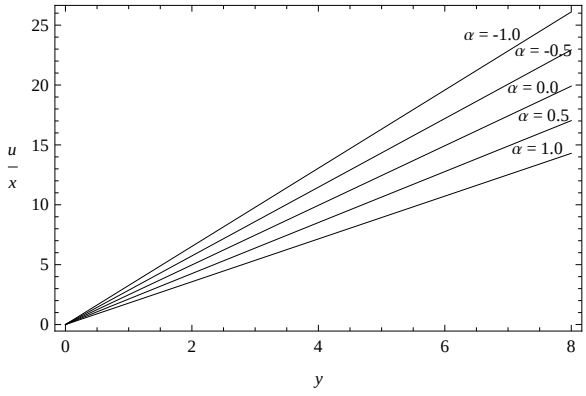

Figure 4: Shear stress profiles over a range of α at $N = 0.5$, $R_e = -1$ and $R = 0.5$

We noticed that, the wall shear stress decreases as the Reynolds number R_e increases, see Table 13.

Table 7: Comparison between analytical and numerical solutions for shear stress τ_ω at $x = 2$ for $N = 0.5$ and $\alpha = -1$.

	Analytical Method	Numerical Method	Percentage Error (%)
$R_e = -1$	6.526164	6.483047	0.665074
$R_e = 1$	-7.731125	-7.755944	0.320003

5. CONCLUSION

In this paper, we have generalized the flow analysis of [4] with the influence of magnetic field and porous medium. The analytical solution for the arising nonlinear problem was obtained by using Lie symmetry technique in conjunction with a second-order double perturbation method. We have studied the effects of magnetic field (N) and porous medium (R) on the self-axial velocity and the results are plotted. We compared the analytical solution with the numerical solution for self-axial velocity at different values of N and R. We found that as N increases the self-axial velocity increases and as R increases the self-axial velocity decreases. Here we have noticed that the analytical results obtained matches quite well with the numerical results for a good range of these parameters. We also noticed that for all cases the self-axial velocity have the similar trend as in [4], that is, the axial velocity approaches a cosine profile. Finally, we observed that when $N = 0$ and R approaches infinity our problem reduces to the problem in [4] and our results (analytical and numerical) also reduce to the results in [4], with the use of first-order double perturbation method.

6. REFERENCES

[1] A.S Berman, Laminar flow in channels with porous walls, J. Appl. Phys. **24**, 1232-1235, 1953.

[2] E.C Dauenhauer and J. Majdalani, Exact self similarity solution of the Navier-Stokes equations for a deformable channel with wall suction or injection, AIAA 3588, 1-11, 2001.

[3] J Majdalani, C Zhou and C.A Dawson, Two-dimensional viscous flow between slowly expanding or contracting walls with weak permeability, J. Biomech. **35**, 1399-1403, 2002.

[4] Y.Z Boutros, A.B Abd-el-Malek, N.A Badran and H.S Hassan, Lie group method solution for two-dimensional viscous flow between slowly expanding

or contracting walls with weak permeability, Appl. Math. Modeling **31**, 1092-1108, 2007.

[5] M. Mahmood, M.A Hossain, S. Asghar and T. Hayat, Application of homotopy pertubation method to deformable channel with wall suction and injection in a porous medium, Int. J. Nonlinear Sci. Numerical Simulation **9**, 195-206, 2008.

[6] S. Asghar, M. Mushtaq and A.H Kara, Exact solutions using symmetry methods and conservation laws for the viscous flow through expanding-contracting channels, Appl. Math. Modeling **32**, 2936-2940, 2008.